Available online at www.sciencedirect.com
ScienceDirect
Cement & Concrete Composites 30 (2008) 544–555
Cement & Concrete Composites
www.elsevier.com/locate/cemconcomp

A design model for punching shear of FRP-reinforced slab-column connections

D.D. Theodorakopoulos [a,*], R.N. Swamy [b]

[a] Department of Civil Engineering, University of Patras, Patras GR 26500, Greece
[b] Department of Mechanical Engineering, University of Sheffield, Mappin Street, Sheffield S1 3JD, England, UK

Received 24 April 2007; received in revised form 10 October 2007; accepted 12 October 2007
Available online 23 October 2007

Abstract

The overall aim of this paper is to develop a unified design method for the punching shear resistance of slab-column connections irrespective of the type of internal reinforcement. In the first part of the paper a design model for the punching shear resistance of concrete slab-column connections reinforced with fibre-reinforced polymers (FRP) is proposed. This design model is based on the authors' theoretical analysis for such slabs, which considers the physical behavior of the connections under load. The effects of the inherent linear brittle response, the lower elastic modulus and the different bond features, as compared to steel, of the FRP reinforcement are all accounted for in the present study. The proposed model does not incorporate any fitting factors to match the theory to the trend of the available FRP slab test results. The excellent agreement between the predicted and published test results should give confidence to engineers and designers in using FRP as a sound structural reinforcement for slab-column connections.

It is then shown that the proposed design model for FRP slabs and the previous model of the authors for steel reinforced slabs are both identical in nature and structure, thus constituting a unified approach to design for punching shear in slabs. On the basis of the unified model comparison and correlation between an FRP slab and a reference steel reinforced slab, confirmed by the available test results, are presented. The unified model also enables the development of a more rational and reliable equivalent steel reinforcement ratio which can be applied to existing code equations for steel reinforced slabs to estimate the punching resistance of FRP-reinforced slabs.

Keywords: Punching strength; Design; Slab-column connection; Fibre-reinforced polymer (FRP)

1. Introduction

The use of FRP reinforcement in practice, especially where the corrosion of steel bars is a concern, is very much hampered by the absence of reliable design methods to determine the ultimate strength of structural elements, especially flat slabs and bridge decks, made with FRP-reinforced concrete. For example, although a few design methods exist to predict the ultimate punching shear strength of slab-column connections reinforced with internal FRP reinforcement, most of these recommendations are either empirically based to fit the available test data [1] or constitute a refinement of various code predictions for steel-reinforced slabs on account of the lower elastic modulus of FRP bars [1–6]. However, the applicability of the above mentioned modified code predictions to FRP-reinforced slabs is questionable because of the differences that exist between FRP and traditional steel reinforcement. FRP compared with steel, has a brittle linear elastic response, as shown in Fig. 1a, but more importantly, it has many different bond features. Punching shear test results reported by various investigators [1,4,5,7–10] reflect these differences, and demonstrate that they affect the ultimate punching load of an FRP slab.

In a recent contribution, Theodorakopoulos and Swamy [11] have proposed a simple analytical model to predict the ultimate punching shear strength of FRP-reinforced

* Corresponding author.
E-mail address: d.d.theod@upatras.gr (D.D. Theodorakopoulos).

0958-9465/$ - see front matter © 2007 Elsevier Ltd. All rights reserved.
doi:10.1016/j.cemconcomp.2007.10.003

Nomenclature

b_o	critical perimeter for punching shear-capacity evaluation, ACI
b_p	critical perimeter for punching-shear capacity evaluation (BS 8110, present study)
d	effective flexural depth of slab
E_s	elastic modulus of steel
E_f	elastic modulus of FRP
f'_c	specified cylinder concrete strength
f_{cm}	mean cylinder compressive concrete strength
f_{ct}	tensile concrete strength
f_{cu}	concrete cube strength, $f_{cu} = f'_c/0.80$
f_f	FRP stress
f_{fu}	ultimate tensile strength of FRP
f_{fud}	ultimate tensile strength of FRP for design purposes, equal to $E_f \times 0.0105$
f_s	steel stress
f_y	steel yield stress
k	factor for the neutral axis depth
k_1	maximum concrete stress block parameter
k_f	reduction factor for FRP reinforcement strain
N	Coefficient
V_c	nominal shear resistance of a flat slab (codes' provisions)
V_{flex}	shear force at ultimate flexural capacity (FRP slabs)
V_{tf}	ultimate test punching strength (FRP slabs)
V_{uf}	ultimate theoretical punching strength (FRP slabs)
V_{ufd}	ultimate design punching strength (FRP slabs)
V_{usd}	ultimate design punching strength (steel slabs)
$(X)_f$	combined neutral axis depth (FRP slabs)
$(X_f)^*_f$	depth of compression zone of the flexural section (FRP slabs-perfect bond)
$(X_f)_f$	depth of compression zone of the flexural section (FRP slabs bond-slip)
X_s	depth of compression zone of the shear section (steel slabs and FRP slabs)
α_s	parameter equal to $\rho_s f_y/0.145\, f_{cu}$ (steel slabs)
α_f	parameter equal to $\rho_f f_{fud}/0.145\, f_{cu}$ (FRP slabs)
ε_{cu}	ultimate concrete compressive strain
ε^*_f	FRP strain (perfect bond, strain compatibility)
ε_f	FRP strain (bond-slip)
ε_{fu}	ultimate tensile FRP strain
ε_{fud}	ultimate tensile FRP strain for design purposes, equal to 0.0105
ε_s	steel strain
ε_{sc}	steel strain of the characteristic slab equal to 0.0105
ε_y	steel yield strain
θ	angle of failure surface
λ_s	parameter equal to f_s/f_y (steel slabs)
λ_f	parameter equal to f_f/f_{fud} (FRP slabs)
ξ_s	depth correction factor equal to $(100/d)^{1/6}$
ρ_s	tension steel reinforcement ratio
ρ_f	FRP reinforcement ratio
ρ_{fb}	balanced FRP reinforcement ratio (perfect bond)

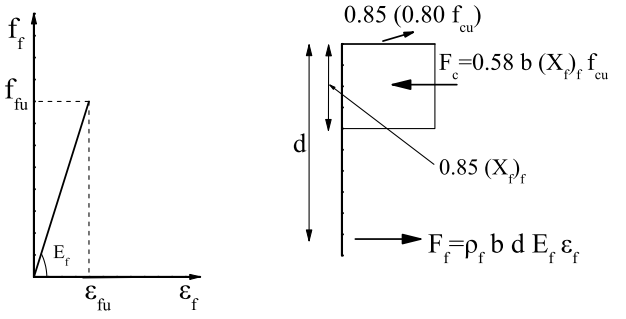

(a) FRP stress-strain response (b) Assumed concrete stress block

Fig. 1. Section force equilibrium.

slab-column connections. The model is based on the physical behavior of the connections under load, and determines the depth of the compression zone to account for the FRP elastic modulus, tensile strength and bond characteristics. The determination of the depth of the compression zone is usually a major obstacle to any satisfactory theory for the ultimate strength in shear.

The overall objective of this paper is to present a simple and reliable design method, accounting for determining the shear capacity of FRP-reinforced slab-column connections at ultimate load. The uniqueness of the proposed model lies on the way it is developed, and it is shown that this model is identical in nature and structure to that used for the design of steel reinforced concrete slabs failing in punching shear. This fact offers engineers an unified design approach for the design of these structural members, irrespective of whether the internal reinforcement is made of steel or FRP. Based on the unified design model comparisons and correlation between the punching shear strengths of an FRP slab and a reference steel slab are presented. In addition, a rational and reliable equivalent steel reinforcement ratio to estimate the punching shear strength of an FRP slab from existing code provisions for a steel reinforced slab is derived.

2. Modified code expressions for FRP slabs

To evaluate the punching shear capacity of FRP-reinforced slabs, researchers have modified the code equations for steel-reinforced slabs of ACI 318-05 [12] and BS 8110-97 [13], given below, to account for the lower elastic modulus of FRP reinforcement. In what follows, all quantities

are in metric units, i.e., strength in N, stresses in MPa, elastic moduli in GPa and dimensions in mm.

According to ACI 318-05 [12] the punching shear resistance of an interior square column steel-reinforced flat slab, in the absence of flexural reinforcement as an influential parameter, is given as

$$V_c^{ACI} = 0.33\sqrt{f'_c}\,b_o d \tag{1}$$

where f'_c is the specified cylinder compressive strength of concrete, b_o is the perimeter at the critical section located at 0.5 d away from the column face and d is the average effective slab flexural depth.

In BS 8110-97 [13], for steel reinforced slabs, V_c is calculated as

$$V_c^{BS} = 0.79(100\rho_s)^{1/3}(f_{cu}/25)^{1/3}(400/d)^{1/4}b_p d \tag{2}$$

where f_{cu} is the cube concrete compressive strength, b_p is the rectangular, regardless of the column shape, critical perimeter located at 1.5 d away from the column face and ρ_s is the steel reinforcement ratio. Based on these equations the following modifications have been proposed for FRP slabs.

El-Ghandour, Pilakoutas and Waldron [2] modified the ACI code equation by introducing the term $(E_f/E_s)^{1/3}$, where E_f and E_s are the modulus of elasticity of FRP and steel, respectively. Thus, Eq. (1) for FRP-reinforced slabs becomes,

$$V_{c,EL}^{ACI} = 0.33\sqrt{f'_c}(E_f/E_s)^{1/3}b_o d \tag{3}$$

The Institution of Structural Engineers [3] recommended the use of an equivalent area of steel in the BS 8110 equation, Eq. (2), by multiplying the actual area of the FRP reinforcement, ρ_f, by the modular ratio

$$\rho_s = \rho_f E_f/E_s \tag{4a}$$

which implies that, given the structure of Eq. (2), the Code equation is again multiplied by the term $(E_f/E_s)^{1/3}$.

El-Ghandour et al. [4] proposed a new modification of Eq. (2), based on their experimental work of FRP flat slabs. According to this approach the equivalent area of steel is obtained as in Eq. (4a), multiplied by a strain correction factor, as shown below:

$$\rho_s = \rho_f(E_f/E_s)(0.0045/\varepsilon_y) \tag{4b}$$

where 0.0045 is the proposed strain limit for FRP reinforcement and ε_y is the steel yield strain. Thus, Eq. (2) for FRP slabs becomes,

$$V_{c,EL}^{BS} = 0.79[100\rho_f(E_f/E_s) \times (0.0045/\varepsilon_y)]^{1/3}(f_{cu}/25)^{1/3}(400/d)^{1/4}b_p d \tag{4}$$

Matthys and Taerwe [5] proposed the following equation, for two-way slabs reinforced with FRP bars or grids, as a modification of BS 8110 equation:

$$V_{c,MT}^{BS} = 1.36[100\rho_f(E_f/E_s)]^{1/3}f_{cm}^{1/3}(1/d)^{1/4}b_p d \tag{5}$$

where f_{cm} is the mean cylinder concrete compressive strength at 28 days.

Furthermore, Ospina, Alexander and Cheng [1] proposed an empirical equation, based on Eq. (5), given by

$$V_{c,0AC} = 2.77(\rho_f f'_c)^{1/3}(E_f/E_s)^{1/2}b_p d \tag{6}$$

It can be seen that in Eq. (6) the effect of modular ratio E_f/E_s is taken as the square root instead of the cube root, in order to produce better results, whereas the scale effect on the punching of slabs with FRP reinforcement is omitted, since this effect was reported not to be evident based on the available FRP test results [1].

A comprehensive review on the reliability of most of the above mentioned predictive equations of test results for FRP-reinforced slabs can be found in Ospina et al. [1]. They reported that among the punching shear strength estimators considered, the modified expression (Eq. (5)) of the BS 8110-97 equation is clearly superior with an average test-to predicted strength ratio of the available test results of 1.17 and a standard deviation of 0.156. However, this equation significantly underestimates the strength of the six slabs reinforced with Carbon FRP of series C1, C2 and C3 tested by Matthys and Taerwe [5], with the average test-to-predicted ratio being 1.40.

More recently, Ospina [6] proposed the following equation for predicting the punching capacity of two-ways slabs reinforced with either steel or FRP bars

$$V_{c,O} = N\sqrt{f'_c}\,b_o kd \tag{7a}$$

where N is a constant equal to 5/6 (for f'_c in MPa, b_o in mm and d in mm). The term kd is the depth of the neutral axis assuming elastic, cracked conditions, where

$$k = \left[\left(\frac{E}{E_c}\rho\right)^2 + 2\frac{E}{E_c}\rho\right]^{1/2} - \frac{E}{E_c}\rho \tag{7b}$$

where $E = E_s$ and $\rho = \rho_s$ for steel slabs, $E = E_f$ and $\rho = \rho_f E_f/E_s$ for FRP slabs, and E_c is the modulus of elasticity of concrete. It can be seen that Eq. (7), in essence, constitutes a modification of the ACI 318 [12] equation through the introduction of the factor k, which represents the effect of the slab reinforcement ratio, steel or FRP. Nevertheless, Eq. (7) is still a conservative predictor when applied to available FRP slab test results [6].

3. Analytical model for FRP slabs

According to the theory of Theodorakopoulos and Swamy [11] the ultimate punching shear strength of FRP-reinforced concrete slabs, accounting for the scale effect, is given as

$$V_{uf} = f_{ct}\cot\theta\,\xi_s b_p (X)_f \tag{8}$$

where

$$(X)_f = \frac{2X_s(X_f)_f}{X_s + (X_f)_f} \tag{8a}$$

$$X_s = 0.25d \tag{8b}$$

In the equations above, $f_{ct} = 0.27 f_{cu}^{2/3}$ and f_{cu} are the tensile and cube compressive strength of concrete, respectively; θ is the mean angle of the failure surface taken as 30°, $\xi_s = (100/d)^{1/6}$ is the scale effect factor, and b_p is the critical perimeter of BS 8110 defined in Eq. (2). Furthermore, X_s, which is independent of the material properties, and $(X_f)_f$ are the neutral axis depths for critical shear section and critical flexural section, respectively. $(X)_f$ is taken as the harmonic mean of X_s and $(X_f)_f$, and represents the combined neutral axis depth of the slab as explained in Refs [14,15]. Eq. (8a) for $(X)_f$ expresses, in effect, that the governing failure load under punching shear is due to the complex moment–shear interaction where punching is considered as a form of combined shearing and splitting, occurring without crushing, but under complex three dimensional stresses [14].

4. Proposed design equation for FRP-reinforced slabs

For the purpose of evaluating the design punching shear strength of FRP-reinforced slab-column connections, the calculation of the neutral axis depth of the flexural section, $(X_f)_f$, at failure, can follow a procedure similar to that proposed for the steel-reinforced slabs in Theodorakopoulos and Swamy [14]. Thus, adopting, for the sake of simplicity, the rectangular concrete stress block associated with ACI 318 (Fig. 1b) where the term $0.80 f_{cu}$ represents the cylinder compressive strength of concrete and using the equilibrium equations, one obtains

$$(X_f)_f = \frac{1}{0.58}\frac{\rho_f f_f}{f_{cu}} d = \frac{\rho_f E_f \varepsilon_f}{0.145 f_{cu}}(0.25d) \tag{9}$$

where $\varepsilon_f = f_f/E_f$ and f_f are the actual strain and stress of FRP reinforcement, respectively.

To evaluate the FRP strain ε_f in Eq. (9) the analysis due to Theodorakopoulos and Swamy [11] is employed. This procedure assumes that, because of the bond-slip failure that occurs at the final stages of failure of tested flat slabs, the actual FRP strain ε_f is a fraction of the FRP strain ε_f^*, calculated on the assumptions of perfect bond and strain compatibility, i.e.,

$$\varepsilon_f = k_f \varepsilon_f^* \tag{10a}$$

or

$$\frac{\varepsilon_f}{\varepsilon_{fu}} = k_f \frac{\varepsilon_f^*}{\varepsilon_{fu}} \quad \text{with } k_f = 0.55 \tag{10b}$$

Thus, the introduction of the coefficient k_f in Eq. (10) reflects the bond characteristics of the FRP reinforcement whereas the assigned value of 0.55 has been based on information reported by Ospina et al. [1] from tests on flat slabs reinforced with glass fibre polymer reinforcement. Furthermore, based on equilibrium of forces in the flexural section, it has been shown [11] that the FRP strain ε_f^*, normalized with respect to ultimate FRP strain ε_{fu}, can be related to the normalized FRP reinforcement ratio ρ_f/ρ_{fb} by

$$\frac{\rho_f}{\rho_{fb}} = \left(\frac{\varepsilon_{cu}}{\varepsilon_{cu}+\varepsilon_f^*}\frac{0.58 f_{cu}}{E_f \varepsilon_f^*}\right) \Big/ \left(\frac{\varepsilon_{cu}}{\varepsilon_{cu}+\varepsilon_{fu}}\frac{0.58 f_{cu}}{E_f \varepsilon_{fu}}\right) = \frac{\varepsilon_{cu}/\varepsilon_{fu}+1}{\varepsilon_{cu}/\varepsilon_{fu}+\varepsilon_f^*/\varepsilon_{fu}}\frac{1}{\varepsilon_f^*/\varepsilon_{fu}} \tag{11a}$$

Thus, solving Eq. (11a) with respect to $\varepsilon_f^*/\varepsilon_{fu}$ and making use of Eq. (10b) one receives

$$\frac{\varepsilon_f^*}{\varepsilon_{fu}} = \frac{-\varepsilon_{cu}/\varepsilon_{fu} + \sqrt{(\varepsilon_{cu}/\varepsilon_{fu})^2 + 4(1+\varepsilon_{cu}/\varepsilon_{fu})/(\rho_f/\rho_{fb})}}{2} \tag{11b}$$

$$\frac{\varepsilon_f}{\varepsilon_{fu}} = k_f \frac{-\varepsilon_{cu}/\varepsilon_{fu} + \sqrt{(\varepsilon_{cu}/\varepsilon_{fu})^2 + 4(1+\varepsilon_{cu}/\varepsilon_{fu})/(\rho_f/\rho_{fb})}}{2} \tag{11c}$$

In the above, ε_{cu} is the specified value of the concrete compressive strain at ultimate and ρ_{fb} is the FRP reinforcement ratio at balanced conditions, that is, an FRP ratio where concrete crushing and FRP rupture occur simultaneously. The ρ_{fb} ratio, the value of which depends on the ultimate FRP strain ε_{fu} considered, is calculated on the assumptions of perfect bond
between FRP and concrete, and strain compatibility conditions.

The effectiveness of using the normalized ratios $\varepsilon_f^*/\varepsilon_{fu}$, $\varepsilon_f/\varepsilon_{fu}$ and ρ_f/ρ_{fb} in Eqs. (11b and c) has been explained in Theodorakopoulos and Swamy [11] and the main conclusions drawn are summarized as follows:

1. The variation of $\varepsilon_f^*/\varepsilon_{fu}$ versus ρ_f/ρ_{fb} is almost independent for a wide range of ε_{fu} (0.0105, 0.0150 and 0.0195) and ε_{cu} (0.0030 and 0.0035) values considered, for the whole range of $\rho_f/\rho_{fb} > 1$. For $\rho_f/\rho_{fb} \leqslant 1$, under the assumption of perfect bond, FRP failure governs and, therefore $\varepsilon_f^*/\varepsilon_{fu} = 1$.
2. Similarly, the variation of $\varepsilon_f/\varepsilon_{fu}$ versus ρ_f/ρ_{fb} (following the slip behavior between FRP and concrete) is again almost independent for the wide range of ε_{fu} and ε_{cu} values mentioned above. This in simple words means that, whereas the values of ratio $\varepsilon_f/\varepsilon_{fu}$ are different for various values of ε_{fu} used, the value of the actual FRP strain ε_f is maintained nearly constant. This conclusion is of great importance and it will be used in the development of the proposed design model for FRP slabs in the next section.
3. Under the condition of bond-slip, Eq. (11c), the new ratio ρ_f/ρ_{fb} that defines the limit of the flexure mode of an FRP-reinforced concrete slab is approximately equal to 0.33, instead of 1.00 for the case of perfect bond, for any value of ε_{fu} considered (ρ_f/ρ_{fb} ranges from 0.34 to 0.32 for $\varepsilon_{fu} = 0.0105$–$0.0195$).
4. The above mentioned value of $\rho_f/\rho_{fb} = 0.33$ depends only on the selected value of $k_f = 0.55$ and increases with increasing value of k_f i.e., if FRP reinforcement with better bond features is used.

4.1. FRP design equation for punching shear

The foregoing considerations provide sufficient background to allow the formulation of the FRP design model, thus reflecting the structural behavior of the flat slab systems and ensuring generality without any loss in accuracy. Thus, the values adopted in the present study for the concrete compressive strain at ultimate and for a reference value of the ultimate FRP strain (any value could be used) are given as

$$\varepsilon_{cu} = 0.0035, \quad \varepsilon_{fud} = 0.0105 (= 3\varepsilon_{cu}) \text{ and } f_{fud} = E_f \varepsilon_{fud} \tag{12}$$

Fig. 2, based on these values, shows the relationship between $\varepsilon_f^*/\varepsilon_{fud}$ or $\varepsilon_f/\varepsilon_{fud}$ and the ratio ρ_f/ρ_{fb}. It can be seen that, as mentioned previously, for $\rho_f/\rho_{fb} > 0.33$ concrete crushing in the flexural section of a flat slab governs, whereas for $\rho_f/\rho_{fb} \leqslant 0.33$ FRP rupture governs.

By introducing the parameters α_f and λ_f defined as

$$\alpha_f = \frac{\rho_f f_{fud}}{0.145 f_{cu}} = \frac{\rho_f E_f \varepsilon_{fud}}{0.145 f_{cu}} \tag{13a}$$

and

$$\lambda_f = \frac{f_f}{f_{fud}} \text{ or } \lambda_f = \frac{\varepsilon_f}{\varepsilon_{fud}} = k_f \frac{\varepsilon_f^*}{\varepsilon_{fud}} \tag{13b}$$

the combined neutral axis depth $(X)_f$ Eq. (8a), on account of Eqs. (9) and (13), is expressed as

$$(X)_f = \frac{2\alpha_f \lambda_f}{1 + \alpha_f \lambda_f} (0.25\text{d}) \tag{14}$$

The coefficient λ_f in Eq. (13b) indicates the stress or strain at which the FRP reinforcement works at failure stages. It is obvious that λ_f is always less than unity for slabs with $\rho_f/\rho_{fb} > 0.33$, which means $\varepsilon_f < \varepsilon_{fud}$. It is to be pointed out that, even though, the calculated values of α_f and λ_f depend on $\varepsilon_{fud} = 0.0105$, their product $\alpha_f\lambda_f = \rho_f E_f \varepsilon_f / 0.145 f_{cu}$ is independent of any value of ε_{fud} that could be used. This means that the value of ε_{fud} is not an influential parameter of the combined neutral axis depth in Eq. (14) and, therefore, of the design punching strength derived below.

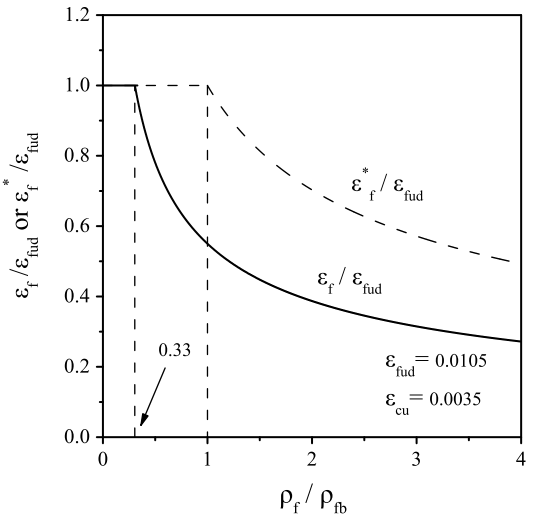

Fig. 2. Variation of the normalized FRP strain $\varepsilon_f/\varepsilon_{fud}$ (bond-slip) versus ρ_f/ρ_{fb} value: $\varepsilon_{fu} = \varepsilon_{fud} = 0.0105$.

From the last expression it can be seen that if $\alpha_f\lambda_f = 1.00$, then $(X)_f = 0.25$ d, which implies, with the aid of Eq. (8b), that for this particular FRP slab the depths of the neutral axis for both the shear and flexural sections are equal to 0.25 d. Such a slab is defined as an "FRP control slab". In addition, one can easily conclude from Eq. (14) that the combined neutral axis depth of an FRP slab decreases, not in a proportional way, with decreasing value of $\alpha_f\lambda_f$.

4.2. Evaluation of coefficient λ_f

On substituting Eq. (13a) into Eq. (11a) and making use of Eq.(12), one obtains that the ratio ρ_f/ρ_{fb} is equal to α_f, i.e.,

$$\frac{\rho_f}{\rho_{fb}} = \alpha_f \quad (\text{for } \varepsilon_{cu} = 0.0035 \text{ and } \varepsilon_{fud} = 0.0105) \tag{15}$$

and, therefore, in what follows, all comments mentioned previously for ρ_f/ρ_{fb}, are also valid for α_f.

The unknown as yet value of λ_f in Eq. (13a) can be calculated for design purposes on account of Eqs. (11c)–(12) and (15), as follows:

$$\lambda_f = \frac{\varepsilon_f}{\varepsilon_{fu_d}} = \frac{k_f}{6}\left(-1 + \sqrt{1 + 48/\alpha_f}\right) < 1 \quad \text{for } \alpha_f > 0.33 \tag{16}$$

From the above, it is apparent that the adopted value of $\varepsilon_{fud} = 0.0105$ in Eq. (12) is fully documented by the simplicity of the relationships between ρ_f/ρ_{fb} and α_f in Eq. (15) and λ_f and α_f in Eq. (16).

In the light of the above considerations, Eq. (8) can take the form

$$V_{ufd} = \frac{1}{2} 0.234 f_{cu}^{2/3} (100/\text{d})^{1/6} b_p \frac{2\alpha_f \lambda_f}{1 + \alpha_f \lambda_f} d \quad \text{for } \alpha_f > 0.33 \tag{17}$$

which, in conjunction with expressions (13a) and (16), is the design prediction equation for the ultimate punching strength of FRP-reinforced concrete slab-column connections.

Eqs. (16) and (17), due to Eq. (15), are obviously valid for $\alpha_f > 0.33$ since (i) for $\alpha_f \leqslant 0.33$ FRP rupture governs and (ii) the proposed FRP design model is intentionally restricted to the case where the punching shear capacity is less than the shear force at the flexural capacity of a slab. However, the application of Eq. (17) to test slabs with $\alpha_f \leqslant 0.33$, and reported to have failed by a mixed failure mode, that is, flexure – punching or punching – flexure might be justified. In such a case, the value of $\lambda_f = \varepsilon_f/\varepsilon_{fud}$ is obviously calculated on the basis of $\varepsilon_f = \varepsilon_{fu}$, irrespective of whether the specified FRP strain ε_{fu} is less or greater

than the reference FRP strain $\varepsilon_{fud} = 0.0105$, since in a real test slab the FRP reinforcement experiences strains up to the tensile strain at ultimate, ε_{fu}.

4.3. Verification of test results and discussion

The proposed design equation has been applied to predict the punching shear capacity of 28 FRP-reinforced concrete slabs reported in the literature. The geometry of the tested slabs, the material properties, the analysis and the results are shown in Table 1. It can been seen that the slabs analyzed cover many variables that influence punching shear behavior, such as, size of loaded area, effective depth of slab, concrete strength, FRP reinforcement ratio and, very importantly, different types of FRP reinforcement with varied manufacturing processes, elastic modulus and ultimate tensile strength. For the proposed design model the predicted-to test punching shear strength ratio is 0.934 with a standard deviation of 0.102. The latter is much less than 0.150, which is generally acceptable from a structural point of view. Thus, the design model appears to be equally reliable and consistent as the authors' proposed theoretical analysis [11], and compares favourably to existing design models for FRP slabs [1,5,6].

It should be pointed out that the proposed design model, based on the moment–shear interaction, reflects the physical behavior of an FRP-reinforced concrete slab-column connection under load. It is derived entirely from basic engineering principles and considers the failure mechanism of FRP-reinforced slabs, and in particular, it incorporates, through the coefficient k_f used for the calculations of the actual FRP strain ε_f and the coefficient λ_f, the bond-slip behavior between FRP bars and concrete. The latter plays a dominant role in the failure process of all FRP-reinforced concrete test slabs [1,5,10], and therefore, there is a need for continuing research on the quality of bond between each type of FRP reinforcement and concrete to confirm the value of k_f on a broader basis. For example, referring back to Table 1, it can be observed that the proposed design model underestimates considerably the punching failure load for series C1, C2 and C3 in Matthys and Taerwe [5] tests, with the average of predicted-to-test

Table 1
Predicted design loads compared with FRP test punching strengths

Ref.	Slab	No[a]	c[b] (mm)	d (mm)	f_{cu}[c] (MPa)	ρ_f (%)	f_{fu} (Mpa)	E_f (GPa)	ε_{fu} (×10e3)	V_{tf} (kN)	α_f[d]	λ_f	$\alpha_f \lambda_f$	V_{ufd} (kN)	V_{ufd}/V_{tf}
		1	2	3	4	5	6	7	8	9	10	11	12	13	14
Ahmad et al. [7]	CFRC-SN1	1	75	61	53.0	0.95	1330	113.0	11.8	93	1.47	0.44	0.65	88.6	0.953
	CFRC-SN2	2	75	61	55.7	0.95	1330	113.0	11.8	78	1.40	0.45	0.63	90.4	1.160
	CFRC-SN3	3	100	61	48.7	0.95	1330	113.0	11.8	96	1.60	0.42	0.67	93.8	0.977
	CFRC-SN4	4	100	61	45.7	0.95	1330	113.0	11.8	99	1.70	0.40	0.69	91.3	0.922
Banthia et al. [8]	I	5	100	55	51.3	0.31	1200	100.0	12.0	65	0.44	0.87	0.38	57.5	0.885
	II	6	100	55	66.1	0.31	1200	100.0	12.0	61	0.34	1.00	0.34	62.6	1.025
Matthys and Taerwe [5]	C1	7	150	96	45.9	0.29	1690	91.8	18.4	181	0.42	0.89	0.37	138.5	0.765
	C1′	8	230	96	46.6	0.29	1690	91.8	18.4	189	0.41	0.90	0.37	164.6	0.871
	C2	9	150	95	44.6	1.05	1340	95.0	14.1	255	1.62	0.42	0.67	197.4	0.774
	C2′	10	230	95	45.4	1.05	1340	95.0	14.1	273	1.59	0.42	0.67	235.5	0.863
	C3	11	150	126	42.3	0.52	1350	92.0	14.7	347	0.82	0.62	0.50	243.9	0.703
	C3′	12	230	126	42.9	0.52	1350	92.0	14.7	343	0.81	0.62	0.50	282.4	0.823
	CS	13	150	95	40.8	0.19	2300	148.0	15.6	142	0.50	0.81	0.41	133.3	0.939
	CS′	14	230	95	41.5	0.19	2300	148.0	15.6	150	0.49	0.82	0.40	158.8	1.059
	H1	15	150	95	147.5	0.64	665	37.3	17.8	207	0.12	1.70	0.20	180.5	0.872
	H2	16	150	89	44.8	3.78	555	40.7	13.6	231	2.49	0.32	0.80	198.5	0.859
	H2′	17	80	89	44.9	3.78	555	40.7	13.6	171	2.48	0.32	0.80	165.3	0.967
	H3	18	150	122	40.1	1.21	640	44.8	14.3	237	0.98	0.56	0.54	235.6	0.994
	H3′	19	80	122	40.1	1.21	640	44.8	14.3	217	0.98	0.56	0.54	203.6	0.938
EL-Ghandour et al. [10]	SG1	20	200	142	41.6	0.22	600	45.0	13.3	170	0.17	1.27	0.22	168.8	0.993
	SC1	21	200	142	43.4	0.18	1000	110.0	9.1	229	0.33	0.87	0.29	215.7	0.942
	SG2	22	200	142	58.2	0.47	600	45.0	13.3	271	0.26	1.15	0.30	273.8	1.010
	SG3	23	200	142	37.9	0.47	600	45.0	13.3	237	0.40	0.91	0.37	238.4	1.006
	SC2	24	200	142	37.0	0.43	1000	110.0	9.1	317	0.93	0.57	0.53	302.6	0.955
Ospina et al. [1]	GFR-1	25	250	120	36.9	0.73	663	34.0	19.5	217	0.49	0.82	0.40	210.8	0.971
	GFR-2	26	250	120	36.1	1.46	663	34.0	19.5	260	1.00	0.55	0.55	257.3	0.990
	NEF-1	27	250	120	46.9	0.87	566	28.4	19.9	206	0.38	0.94	0.36	228.3	1.108
Zaghloul & Razaqpur [9]	–	28	250	75	56.3	1.00	1700	100.0	17.0	234	1.29	0.48	0.61	195.1	0.834
											Average ratio				**0.934**
											Standard deviation				**0.102**

[a] Numbering of slabs.
[b] Column width: square or diameter.
[c] Concrete strength at testing time.
[d] $\alpha_f = \rho_f \times E_f \times 0.0105/0.145\, f_{cu}$.

strength ratios for these six slabs (from No 7 to No 12) being 0.800. This underestimation may be explained in terms of the possibly better bond characteristics of the particular type of reinforcement used in series C (Carbon NEFMAC) than those on which the value of $k_f = 0.55$ was based (Glass FRP) [11]. Thus, applying the proposed design model to slabs of series C using an increased value of k_f by 30%, i.e., $k_f = 1.30 \times 0.55 = 0.715$, it can be found (not shown here) that a much better agreement between predicted-to test strengths for these six slabs is obtained with the new average of ratios of 0.945. This indicates an average increase in punching strength of only 18% (0.945/0.800 = 1.18), and this is due to the fact that, whereas the contribution of the critical flexural section to ultimate punching resistance increases proportionally with increasing value of k_f (Eqs. (9) and (10b)), the contribution of the critical shear section remains constant, ($X_s = 0.25$ d).

The proposed design model does not incorporate any empirical factors to match the predictions to available FRP slab test results. As a result, the proposed design Eq. (17) is not subject to any limitation as far as the material properties and reinforcement ratio are concerned. Indeed, although the available test results are limited, it is observed from Table 1 that the design predictions are close to test strengths even for slab H1 made with high strength concrete ($f_{cu} = 147.5$ MPa) and slabs H2/H2′ reinforced with a large amount of FRP reinforcement ($\rho_f = 3.78\%$). It is also worth stating, based on the development of the model, that any difference between the ultimate strength and/or the elastic modulus of the FRP reinforcement specified by the manufacturer and test properties of FRP is not a concern for the design prediction of the punching failure load, except for slabs with low flexural reinforcement, as explained below.

Thus, it is of interest to mention the design predictions for FRP test slabs reinforced with values of α_f equal to or less than 0.33. According to the proposed FRP design model such slabs must fail in flexure. In fact, most of these slabs in Table 1, such as H1, SG1, SC1 and SG2 have been reported to have failed either by a mixed (flexure-punching) or by a bond-slip mode. Normally, the comparisons between the model's prediction and test loads for these slabs should not be included in Table 1, since the model presented here is intentionally restricted for the cases where punching shear capacity is less than the shear force, V_{flex}, at the ultimate flexural capacity of the slab. However, because of the mode of failure of the above mentioned slabs, the shear capacities of the slabs can be considered only slightly above the test failure loads, and therefore a comparison between design and test results can be made. This is justified by the V_{ufd}/V_{tf} ratios being 0.872, 0.993, 0.942 and 1.010 for test slabs H1, SG1, SC1 and SG2, respectively. It should be noted that for these slabs, because of their mode of failure, the value of λ_f (column 11, Table 1) has been calculated, as explained in a previous section, on the basis of Eq. (13b) and for $\varepsilon_f = \varepsilon_{fu}$. Finally, it is worth noting that for all test slabs shown in Table 1, the calculated values of $\alpha_f\lambda_f$ (column 12) are less than 1.00, as a consequence of the bond-slip behavior of FRP reinforcement. This indicates that the neutral axis depth of their flexural section, on account of Eqs. (8b) and (14), is less than that of the FRP control slab, i.e., less than 0.25 d, thus verifying the fact that flexural crack heights in FRP-reinforced members are expected to be larger than those in steel reinforced members.

In what follows, the authors' design equation for steel-reinforced concrete slabs [14] is briefly presented and the two models are compared. In addition, a new equation of the equivalent steel ratio is proposed on the basis of equal design predictions for two slabs identical in all respects but the type of reinforcement.

5. Design model for steel slabs

For the two-way normal concrete slabs reinforced with steel bars, the following design equation has been proposed for the ultimate design strength, V_{usd} (Theodorakopoulos and Swamy) [14]. By defining,

$$\alpha_s = \frac{\rho_s f_y}{0.145 f_{cu}} \quad \text{and} \quad \lambda_s = \frac{f_s}{f_y} \tag{18}$$

with

$$\lambda_s = \begin{cases} 1.60 - 0.75\alpha_s & \text{for } 0.20 \leqslant \alpha_s \leqslant 0.50 \\ 1.35 - 0.25\alpha_s & \text{for } 0.50 \leqslant \alpha_s \leqslant 1.00 \\ 1.20 - 0.10\alpha_s & \text{for } 1.00 \leqslant \alpha_s \leqslant 2.50 \\ 1.30 - 0.14\alpha_s & \text{for } 2.50 \leqslant \alpha_s \leqslant 5.00 \end{cases} \tag{19}$$

then

$$V_{usd} = \frac{1}{2} 0.234 f_{cu}^{2/3} (100/d)^{1/6} b_p \frac{2\alpha_s\lambda_s}{1 + \alpha_s\lambda_s} d \tag{20}$$

In the above, f_s and f_y are the steel stress and the steel yield stress, respectively. Therefore, the coefficient λ_s in Eq. (19) indicates the effectiveness of the steel stress, i.e., the stress at which the tension steel works (either greater or less then f_y) at the ultimate stage of punching. Details of the calculation of λ_s can be found in Ref. [14]. It is again worth noting that the design Eq. (20) for steel-reinforced slabs, based on the authors' theoretical analysis for punching shear of steel-reinforced slabs [15], does not employ any factor estimated empirically from test data. Furthermore, as in the case of FRP slabs, for the particular steel slab for which $\alpha_s\lambda_s = 1$, it is implied that both the neutral axis depths of the shear and flexural sections are equal to 0.25 d, and therefore, such a slab is defined as a "steel characteristic or control slab".

It has been shown that Eq. (20) predicts the steel-reinforced slab test results in a better way than Design Codes with a smaller standard deviation [16]. Furthermore, Ospina et al. (steel slab SR-1) [1] and Matthys and Taerwe (steel slabs R1, R1′, R2 and R3) [5], cast these steel reference slabs for comparison purposes to their FRP-reinforced slabs. Applying Eq. (20) (not shown here) to the above mentioned steel

slabs one can find predicted-to-test strength ratios of 0.945 for slab SR-1 and 0.850 (on the mean) for slabs R1, R1′, R2 and R3. It is to be pointed out that these ratios are of comparable magnitude to those (on the mean) of the corresponding FRP-reinforced slabs of these researchers.

6. A unified model for punching shear

A comparison of the design expressions (16) and (17) and (19) and (20) for FRP-reinforced and steel reinforced slabs, respectively, shows that the two models are identical in nature and structure. Both models include all the key parameters that play an important role on punching shear behavior, such as, size effect, size of the column area, slab effective depth, reinforcement ratio and concrete strength. It is obvious that they differ only in the value of $\alpha\lambda$ – since the parameter $\alpha_f\lambda_f$ expresses the different engineering properties and bond characteristics of the FRP reinforcement, as compared to parameter $\alpha_s\lambda_s$ for steel reinforcement. Also, the term $2\alpha\lambda/(1+\alpha\lambda)$ in both equations expresses the interaction of the two critical sections considered in developing the proposed equations, namely, shear and flexural. As a result of this moment–shear interaction, it can easily be seen from the two design equations that the influences of the steel or FRP ratio and concrete strength on punching shear strength are not isolated and single contributors, as assumed in code equations. Finally, in addition to the above considerations it appears that the design Eqs. (17) and (20) retain the structure and simplicity of various code equations for steel slabs or modified equations for FRP slabs and, therefore, they are easy to apply by researchers and design engineers.

Thus, as a conclusion, it can be said that a simple and reliable unified design model for punching shear strength of slab-column connections, based on sound engineering principles, is possible and applicable to all slabs irrespective of whether the internal reinforcement is made of steel or FRP. Based on the unified model, the punching strengths of an FRP slab and a reference steel slab are easy to compare and correlate, and a new equation of the equivalent steel ratio is proposed in the next section.

6.1. Comparison between FRP and steel slabs (experimental evidence)

Matthys and Taerwe [5], in their systematic FRP-reinforced slab tests, given in Table 1, have compared the strength results with those obtained by the steel reinforced reference slabs R1/R1′, with $c = 150/230$ mm, $d = 90$ mm, $f_{cu} = 41.9$ MPa, $\rho_s = 0.58\%$, $f_y = 500$ MPa, $E_s = 200$ GPa, which imply $\alpha_s = 0.48$ and $\lambda_s = 1.24$, and failure loads of 240/255 kN, respectively. The comparison of test strengths was based on the following general characteristics: the flexural strength which is proportional to $\rho_f f_{fu}$ or $\rho_s f_y$, the equivalent reinforcement ratio $\rho_s = \rho_f E_f/E_s$ given by Eq. (4a) and the flexural stiffness of the section expressed by $\rho_f E_f d^2$ or $\rho_s E_s d^2$ for FRP and steel slabs, respectively. Their general conclusions are briefly summarized here for the sake of completeness.

- FRP-reinforced concrete slabs, such as of series C1 and CS designed with a similar flexural strength as reference slabs of series R1, have significantly lower punching strengths.
- Comparing slabs with similar effective depths and different types of flexural reinforcement, the obtained failure loads are roughly similar for equal equivalent reinforcement ratios $\rho_f E_f/E_s$, such as slabs of series R1, C2 and H2 or of series C1 and CS.
- FRP-reinforced concrete slabs designed with a similar flexural stiffness as steel reference slabs R1/R1′ have similar or higher punching strengths for series C2/C2′ and C3/C3′ and slightly lower punching strengths for slabs H2 and H3.
- Comparing FRP slabs with similar flexural stiffness but with different effective depths and reinforcement ratios, such as C2/C2′ and C3/C3′, the effect of increasing the slab depth on the punching resistance (comparing slabs C1/C3) seems to be more pronounced than the effect of increasing the reinforcement ratio (comparing slabs C1/C2).
- Comparing slab H2 with the steel reference slab R1 of similar flexural stiffness, it is concluded that to obtain similar punching resistance the FRP-reinforced slabs should have an FRP ratio that is sufficiently higher than steel ratio.

Based on the above considerations, it can be said that all three characteristics, namely, flexural strength, equivalent reinforcement ratio and flexural stiffness of the section used by Matthys and Taerwe [5] constitute a good basis for comparison purposes between FRP and steel reinforced flat slabs. However, none of these characteristics accounts for parameters that influence, as indicated by experimental evidence, the structural behavior of a connection, such as moment–shear interaction, slipping of the FRP reinforcement at failure stages and level of the concrete strength value.

6.2. Theoretical comparison between FRP and steel slabs

The comparison and correlation between FRP and steel reinforced concrete slabs of this section have been obtained on the basis of the unified design model presented previously. The case of slabs identical in all respects except the type and percentage of reinforcement and failing in punching shear is examined. One can argue, based on the development of the unified design model, that the expressions of α_f and α_s are the most representative parameters of the problem. Indeed, Eq. (13a) for α_f and Eq. (18) for α_s contain the quantities $\rho_f f_{fu}$ and $\rho_s f_y$ (for flexural strength), $\rho_f E_f$ and $\rho_s E_s$ (for equivalent reinforcement ratio) and, in addition, the concrete strength f_{cu}. Furthermore, coefficients λ_f and λ_s account for the bond between concrete

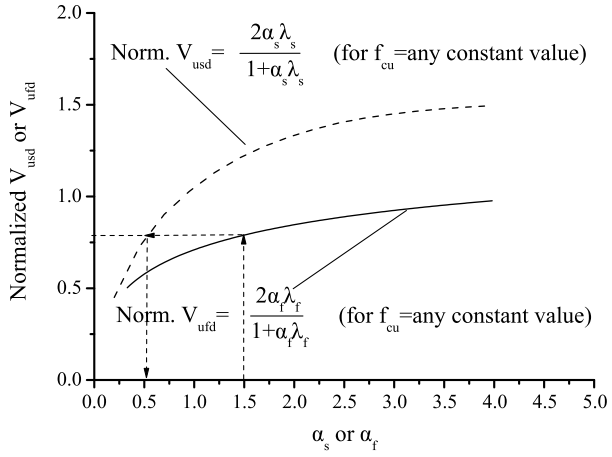

Fig. 3. Variation of the normalized design punching strengths (steel and FRP slabs) versus α_s or α_f: $k_f = 0.55$.

and FRP (slip behavior) and steel reinforcement (perfect bond), respectively.

Fig. 3 shows the variation of the ultimate punching shear strengths, Eqs. (17) and (20), versus α_f and α_s for FRP and steel reinforced slabs, respectively. The strengths are normalized with respect to strength of the FRP or steel control slab (1/2) 0.234 $f_{cu}^{2/3}\xi_s b_p d$, and therefore the obtained variations are valid for any level of the concrete strength value. It can be seen that both variations are similar, as far as the pattern is concerned, and increase monotonically for the whole range of α_f or α_s values, approaching almost a horizontal line at high values of these parameters. This configuration has four implications: two are easy to understand, and the other two are more obscure.

1. FRP and steel slabs with $\alpha_f = \alpha_s$. According to the curves in Fig. 3, FRP-reinforced concrete slabs designed with the same flexural strength ($\rho_f f_{ufd}$) as the reference steel reinforced slab ($\rho_s f_y$), which implies $\alpha_f = \alpha_s$, should have significantly lower punching strengths. This conclusion of the theory is due (i) to the lower elastic modulus of the FRP reinforcement, as compared to steel and (ii) to the bond-slip behavior of the FRP reinforcement ($k_f = 0.55$). If a higher value is assigned in k_f, say 0.715, to reflect the use of FRP reinforcement with better bond characteristics, as Carbon NEFMAC in slabs of series C1, C2 and C3 [5], the predicted punching strengths increase (not shown in Fig. 3), still remaining lower than the predicted strength of the reference steel-reinforced slab. This is fully justified by the test results of Matthys and Taerwe [5], as mentioned before, by comparing the slabs of series C1 and CS with the reference steel slab R1.
2. FRP and steel slabs with equal punching resistances. To obtain equal punching resistances between an FRP slab and a reference steel slab, one can follow the arrows shown in Fig. 3. It is clear that the FRP slab should have an α_f value that is sufficiently higher than α_s for reasons analogous to those of point 1. An example of this are slabs H2 ($\alpha_f = 2.49$) and R1 ($\alpha_s = 0.48$) with comparable magnitude of failure loads, being 231 kN and 240 kN, respectively [5]. This aspect will be explained and discussed in detail in the next section.
3. Effect of increasing reinforcement ratio. Given that α_f and α_s are proportional to ρ_f and ρ_s, respectively, it can be seen from Fig. 3 that the punching resistance of a connection increases with increasing reinforcement ratio, steel or FRP. It is also observed that for a given increased reinforcement ratio either for FRP or steel slabs, its effect on punching strength depends on the rank of the initial value of α_f (ρ_f) or α_s (ρ_s) considered. For example, and referring to steel slabs, it can be found that the percentage increase in punching shear resistance from doubling the steel ratio ρ_s is 42% and 27% for initial values α_s of 0.35 and 1.00, respectively. In addition, this conclusion, given that different initial values of α_s may result from a change of f_{cu}, implies that the level of the concrete strength plays a significant role on the effect of increasing reinforcement ratio. Finally, it should be noted, for the sake of comparison, that according to BS 8110 [13] design equation, Eq. (2), the percentage increase in punching strength when the steel reinforcement ratio is doubled, is constant and equal to 26% ($\sqrt[3]{2} = 1.26$), i.e., independent of the steel ratio the initial slab is reinforced with and the level of the concrete strength.
4. Effectiveness of FRP as compared to steel reinforcement. A close inspection of two variations of punching resistance in Fig. 3 reveals that the increased predicted punching capacity based on equal initial values of α_f and α_s ($\alpha_f = \alpha_s$) and associated with the same increase in flexural reinforcement, is greater for steel than FRP slabs. This result can be attributed to both the lower elastic modulus ($E_f < E_s$) and the bond-slip behavior of the FRP reinforcement, taken into account in developing the proposed FRP design model.

Test results from both FRP and steel reinforced flat slabs fully justify the above mentioned conclusion. For example, referring to slabs GFR-1 and GFR-2 in Table 1, one can find that the test load increased by 20% (260/217 = 1.20) when the FRP reinforcement ratio doubled from 0.73% (initial value of $\alpha_f = 0.49$) to 1.46%. On the other hand, Base [17] reported that the percentage increase in punching resistance from nearly doubling the steel ratio from 0.73% (initial value of $\alpha_s = 0.52$) to 1.63% was 30%, whereas Tolf [18] reported the same average increase 30% when the steel ratio increased from 0.35% (initial value of $\alpha_s = 0.47$) to 0.80%. These test results from steel slabs with comparable values of initial α_s but different initial values of ρ_s verify, in essence, the role of concrete strength, mentioned in point 3 above.

A more in-depth discussion of the effects of flexural reinforcement, reinforcement grade (i.e., yield strength, ultimate tensile strength of FRP bars), bond-slip behavior of

the FRP reinforcement, concentration of reinforcement under the column and concrete strength (normal weight and high strength concrete) on punching strength cannot be accommodated within the length specifications of this paper, and will therefore form the subject matter of another paper.

6.3. Equivalent steel ratio

The equivalent steel reinforcement ratio required to refine the various code predictions for steel-reinforced slabs, when the ultimate design punching shear strength of an FRP-reinforced slab is needed, can easily be estimated on the basis of the above mentioned unified model, as follows.

By equating the design predictions from Eqs. (17) and (20), one obtains

$$\alpha_s\lambda_s = \alpha_f\lambda_f \text{ or } \alpha_s/\alpha_f = \lambda_f/\lambda_s \tag{21}$$

Thus, Eq. (21), with the aid of Eqs. (13a) and (18), after rearranging the terms, yields

$$\rho_s = \rho_f \frac{E_f}{E_s}\frac{\varepsilon_{fud}}{\varepsilon_y}\frac{\lambda_f}{\lambda_s} \quad \text{with } \varepsilon_{fud} = 0.0105 \tag{22}$$

Eq. (22) indicates that, according to the authors' proposed design expressions, the equivalent area of steel reinforcement can be obtained as in Eq. (4b) (it is noted a different value in the strain limit of the FRP reinforcement between Eqs (22) and (4b)) multiplied further by a stress correction factor, expressed by λ_f/λ_s.

The unknown as yet stress factor λ_f/λ_s, which is equal to α_s/α_f, can be determined with the aid of Eqs. (16), (19) and (21), if the value of α_f is known. Fig. 4 shows the variation of both α_s and α_s/α_f with respect to α_f. It is observed that, for equal design predictions of an FRP slab and a reference steel slab, the value of α_s increases, as expected, with increasing α_f, although in a much lesser degree. As a consequence of this, the ratio α_s/α_f decreases from 0.70 for $\alpha_f = 0.33$ to 0.20 for $\alpha_f = 4.55$ at a rather constant rate of decay for high values of α_f. On the other hand, low values of α_f produce high values of the ratio $\alpha_s/\alpha_f = \lambda_f/\lambda_s$ and this can be explained in terms of the yielding behavior of the resulting low value of the equivalent steel ratio. Fig. 4 also shows that, for the whole range of α_f, the ratio $\alpha_s/\alpha_f = \lambda_f/\lambda_s$ is lower than unity due to the bond-slip behavior of the FRP reinforcement. Furthermore, Eqs. (4a) and (4b) indicate that for given material properties ρ_f, f_{cu}, E_f, E_s and ε_y, the equivalent steel ratio, taken as a percentage of the FRP ratio (ρ_s/ρ_f), is constant. However, in the light of the above discussion, it is apparent that, due to Eq. (22), the ratio ρ_s/ρ_f decreases with increasing value of α_f, which implies that even different concrete strengths provide different equivalent steel ratios.

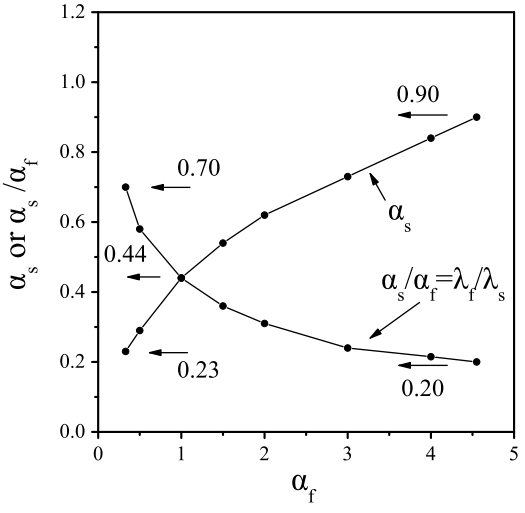

Fig. 4. Relationship between α_s or α_s/α_f values and α_f value for equal design predictions (steel and FRP slabs): $k_f = 0.55$.

Finally, it can be easily found that to obtain values of comparable magnitude for the equivalent steel ratio from Eqs. (4a)–(22) or from Eqs. (4b)–(22) the value of α_f should be around of 4.5 (slabs H2/H2′) and 1.0 (slabs C3/C3′ and H3/H3′), respectively. These results are also shown in Table 2, where the equivalent steel reinforcement ratios according to Eqs. (4a), (4b) and (22), for test slabs in Matthys and Taerwe [5], are given for comparison purposes. One can see that the results of Eq. (22) compare favorably to those of Eqs. (4a and b) for slabs R1 (reference steel slab), C2 and H2, designed, as mentioned previously, with similar effective depths and for roughly equal equivalent reinforcement ratios, and for which the obtained failure loads are of comparable magnitude. It is also of interest to note that for slabs CS/CS′ with a large value of $E_f = 148$ GPa, the equivalent steel reinforcement ratio according to Eq. (22) [$0.28\% = 0.19\% (148/200) \times (0.0105/0.0031) \times (0.30/0.50)$] is higher than the initial FRP ratio, $\rho_f = 0.19\%$, for reasons analogous to those explained above.

Taking the above as a whole, it can be said that the calculation of the equivalent steel ratio on the basis of the unified model, is more reliable than those based on Eqs. (4a) and (4b). In addition to FRP ratio (ρ_f) and modular ratio (E_f/E_s), parameters that significantly influence punching strength, such as reinforcement ultimate stresses

Table 2
Equivalent steel reinforcement ratio

Test slabs[5]	Type of reinforcement	ρ_s or ρ_f (%)	α_s or α_f	V_t (kN)	Equivalent steel ratio (%)		
					Eq. (4a)	Eq. (4b)	Eq. (22)
R1/R1′	Steel	0.58	0.48	240/255	0.58	0.58	0.58
C1/C1′	FRP	0.29	0.42	181/189	0.12	0.17	0.26
C2/C2′	FRP	1.05	1.62	255/273	0.50	0.73	0.58
C3/C3′	FRP	0.59	0.82	347/343	0.24	0.35	0.39
CS/CS′	FRP	0.19	0.50	142/150	0.14	0.20	0.28
H2/H2′	FRP	3.78	2.49	231/171	0.77	1.12	0.71
H3/H3′	FRP	1.21	0.98	237/217	0.27	0.39	0.39

(f_y, f_{fu}, through ε_y and ε_{fud}), bond features of the flexural FRP reinforcement (k_f, through the value of λ_f) and concrete strength (f_{cu}, through the values of α_s and α_f) are all accounted for. It is obvious that the use of the proposed equivalent steel ratio of Eq. (22), to refine the various code predictions for steel reinforced slabs, will provide a reliable estimator for the punching shear strength of FRP-reinforced slabs, only if the code expression used is an accurate predictor for the punching strength of the so-called reference steel slab.

7. Conclusions

The main conclusions derived from this study may be summarized as follows:

1. A design equation, Eq. (17), is developed to predict the ultimate punching shear strength of FRP-reinforced concrete slabs. The approach is based on the authors' theoretical analysis for such slabs, which considers the structural behavior of the connections under load.
2. The proposed design model accounts for the mechanical properties of the FRP reinforcement, which are sufficiently different from those of steel, such as, elastic modulus, ultimate tensile strength and, mainly, the bond characteristics. It, also, incorporates no empirical factors to match the theory to the trend of the available FRP slab test results. As a result, no limits are placed as far as the material properties are concerned.
3. The proposed predictive equation retains the structure and simplicity of the modified code expressions for FRP slabs. In addition, the contribution of the FRP reinforcement ratio and concrete strength on the punching shear strength are both incorporated in a combined way, thus reflecting the dependence of the punching failure load on these interacting variables.
4. The predictions of the proposed design equation are in excellent agreement with the available experimental failure loads of FRP test slabs, reported by various investigators. Also, the proposed model compares favorably to existing design models for FRP slabs, reported in the literature.
5. The proposed design model for FRP slabs and the previous model of the authors for steel reinforced slabs are both identical in nature and structure, and include all the key parameters that significantly influence punching shear behavior. Thus, the two models constitute a unified model to design for punching shear, irrespective of whether the internal reinforcement is made of steel or FRP.
6. With the aid of the unified model a new equation of the equivalent steel ratio is proposed on account of a stress factor for steel and FRP. In addition, the unified model accommodates the comparison and correlation between steel and FRP slabs, verified by experimental results, in a reliable and consistent way.
7. Given the agreement between predicted and test results, it is concluded that the proposed unified model provides a convenient and reliable framework for the punching strength design of slabs reinforced with any type of reinforcement, steel or FRP.

References

[1] Ospina CE, Alexander SDB, Cheng JJR. Punching of Two-Way Concrete Slabs with Fiber-Reinforced Polymer Reinforcing Bars or Grids. ACI Struct J 2003;100(5):589–98.
[2] El-Ghandour AW, Pilakoutas K, Waldron P. New approach for punching shear capacity prediction of fiber reinforced polymer reinforced concrete flat slabs. In: Dolan CW, Rizkalla SH, Nanni A, editors. Proceedings of the fourth international symposium on fiber reinforced polymer reinforcement for reinforced concrete structures, SP-188, American Concrete Institute, Farmington Hills, Mich., 1999. p. 135–44.
[3] Institution of Structural Engineers. Interim guidance on the design of reinforced concrete structures using fibre composite reinforcement. The Institution of Structural Engineers, London, 1999.
[4] El-Ghandour AW, Pilakoutas K, Waldron P. Punching shear behavior and design of FRP RC flat slabs. In: Silfwerbrand J, Hassanzadeh G editors. Proceedings of the international workshop on punching shear capacity of RC slabs, Dedicated to Professor Sven Kinnunen. Stockholm: TRITA-BKN Bulletin 57, 2000. p. 359–66.
[5] Matthys S, Taerwe L. Concrete Slabs Reinforced with FRP Grids. II: Punching Resistance. ASCE J Compos Const 2000;4(3):154–61.
[6] Ospina CE. Alternative Model for Concentric Punching Capacity Evaluation of Reinforced Concrete Two-way Slabs. ACI Concr Int 2005;27(9):53–7.
[7] Ahmad SH, Zia P, Yu TJ, Xie Y. Punching shear tests of slabs reinforced with 3-D Carbon Fiber Fabric. ACI Concr Int 1993;16(6):36–41.
[8] Banthia N, Al-Asaly M, Ma S. Behavior of Concrete Slabs Reinforced with Fiber-Reinforced Plastic Grid. ASCE J Mater Civil Eng 1995;7(4):643–52.
[9] Zaghloul AE, Razaqpur AG. Punching shear behavior of CFRP reinforced concrete flat plates. In: Bruno D, Spadea G, Swamy RN, editors. Proceedings of the international conference on composites in construction, 2003. p. 726.
[10] El-Ghandour AW, Pilakoutas K, Waldron P. Punching Shear Behavior of Fiber Reinforced Polymers Reinforced Flat Slabs: Experimental Study. ASCE J Compos Const 2003;7(3):258–65.
[11] Theodorakopoulos DD, Swamy RN. Analytical Model to Predict the Punching Shear Strength of FRP-Reinforced Concrete Flat Slabs. ACI Struct J 2007;104(3):257–66.
[12] ACI 318-05. Building code requirements for structural concrete and commentary. Farmington Hills (MI): American Concrete Institute, 2005.
[13] British Standards Institution. Structural use of concrete, BS8110: Part 1 – Code of practice for design and construction. London: British Standards Institution, 1997.
[14] Theodorakopoulos DD, Swamy RN. A design method for punching shear strength of steel fiber reinforced concrete. American Concrete Institute, SP-216, Innovations in Fiber-Reinforced Concrete for Value, 2003, p. 181–201.
[15] Theodorakopoulos DD, Swamy RN. Ultimate Punching Shear Strength Analysis of Slab-Column Connections. Cement and Concrete Composites, Special Theme Issue 2002;24(6):509–21.
[16] Theodorakopoulos DD, Swamy RN. Design equations to predict the ultimate punching shear strength of slab-column connections. In:

Brandt A, editor. Proceedings of the international symposium BMC7. Warsaw, 2003.

[17] Base GD. Some tests on the punching shear strength of reinforced concrete slabs. Technical Report TRA/321. Cement and Concrete Association, London 1959.

[18] Tolf P. Plattjocklekens inverkan pabetongplattors ha llfasthet vid genomstansning. Forsok med cikulara platter. Bulletin 146. Stockholm, Department of Structural Mechanics and Engineering, KTH, 1998 [in Swedish with summary in English].